

## NOISE AND BANDWIDTH MEASUREMENTS OF DIFFUSION-COOLED Nb HOT-ELECTRON BOLOMETER MIXERS AT FREQUENCIES ABOVE THE SUPERCONDUCTIVE ENERGY GAP

R.A. Wyss, B.S. Karasik, W.R. McGrath, B. Bumble and H. LeDuc

Center for Space Microelectronics Technology,  
Jet Propulsion Laboratory, California Institute of Technology,  
Pasadena, CA 91109

### ABSTRACT

Diffusion-cooled Nb hot-electron bolometer (HEB) mixers have the potential to simultaneously achieve high intermediate frequency (IF) bandwidths and low mixer noise temperatures for operation at THz frequencies (above the superconductive gap energy). We have measured the IF signal bandwidth at 630 GHz of Nb devices with lengths  $L = 0.3, 0.2,$  and  $0.1 \mu\text{m}$  in a quasioptical mixer configuration employing twin-slot antennas. The 3-dB IF bandwidth increased from 1.2 GHz for the  $0.3 \mu\text{m}$  long device to 9.2 GHz for the  $0.1 \mu\text{m}$  long device. These results demonstrate the expected  $1/L^2$  dependence of the IF bandwidth at submillimeter wave frequencies for the first time, as well as the largest IF bandwidth obtained to date. For the  $0.1 \mu\text{m}$  device, which had the largest bandwidth, the double sideband (DSB) noise temperature of the receiver was 320-470 K at 630 GHz with an absorbed LO power of 35 nW, estimated using the isothermal method. A version of this mixer with the antenna length scaled for operation at 2.5 THz has also been tested. A DSB receiver noise temperature of  $1800 \pm 100$  K was achieved, which is about 1,000 K lower than our previously reported results. These results demonstrate that large IF bandwidth and low-noise operation of a diffusion-cooled HEB mixer is possible at THz frequencies with the same device geometry.

### I. INTRODUCTION

To date, diffusion-cooled hot electron bolometer (HEB) mixers have achieved low receiver noise temperatures at 1,100 GHz<sup>[1]</sup> and 2.5 THz<sup>[2]</sup> and large intermediate frequency (IF) bandwidths<sup>[3]</sup>. Phonon-cooled HEB mixers have also shown very good performance<sup>[4-6]</sup> though the IF bandwidth is ultimately limited by the electron-phonon energy relaxation time. The combination of low-noise and high IF is both desirable and critical for applications in radioastronomy. Unlike the SIS mixer, the HEB mixer works well above the superconductive energy gap frequency ( $f_g \approx 750$  GHz for Nb) which makes it the detector of choice for observational science applications at THz frequencies.

using a 2 mil Mylar beamsplitter. At each frequency point the LO radiation is re-aligned as necessary to maintain a constant pump power level and hence a fixed bias point of the HEB. Since the objective is to observe a large signal bandwidth, narrow-band cooled amplifiers were not used for this measurement. The frequency dependent loss of the microstrip line connecting the HEB chip to the K-connector, the semi-rigid cable used to bring the signal from the 4.2 K stage to the outside of the dewar, the two 30-dB room-temperature Miteq amplifiers, and the input of the spectrum analyzer, were all carefully measured. The product of these losses was used to calibrate the data before extracting the intrinsic frequency dependence of the HEB mixer. The receiver noise temperature was also measured at 630 GHz by the Y-factor method using a similar setup. The monochromatic signal source was replaced with a hot or cold load. These loads are made of a cone-shaped eccosorb foam which was either at room temperature or LN<sub>2</sub> temperature. A 4.2 K cooled HEMT amplifier was used as the first stage for the IF system to amplify the signal from the HEB mixer by ~40 dB, and a bandpass filter with center frequency of 2.180 GHz and bandwidth of 300 MHz was inserted before the two Miteq amplifiers. A power meter was used to measure the IF output.

The receiver performance at THz frequencies is measured using an experimental setup similar to that described Karasik *et al.*<sup>[2]</sup>, and briefly discussed here. The local oscillator source is a CO<sub>2</sub>-pumped far-infrared laser operating on the 118.8  $\mu\text{m}$  (i.e. 2.5 THz) lasing line of methanol gas. The radiation is steered towards the input window of the dewar using two mirrors and a 1 mil thick Mylar beamsplitter. The power level and polarization is controlled using two metal grids which can be rotated relative to each other. The Y-factor is determined by switching between a hot (295 K) and cold load (~95 K). Atmospheric absorption is eliminated in the signal path and part of the LO path by placing the beamsplitter and the temperature loads in a vacuum box mounted to the dewar. The need for a vacuum window on the dewar is hence eliminated and only a Zitex filter<sup>[8]</sup> is mounted on the LN<sub>2</sub>-shield to prevent room-temperature infrared radiation from reaching the mixer block. This minimizes the loss between the hot/cold load and the HEB mixer, and reduces superfluous noise temperature contributions. Thus our system accurately measures the receiver noise temperature without any corrections for atmospheric absorption or windows. The mixer IF output is amplified using a LHe-cooled HEMT amplifier having a gain of ~40 dB with a noise temperature <4.0 K in the frequency band of interest, 1.9 to 2.4 GHz. The IF signal is bandpass limited to 300 MHz, with center frequency of 2.18 GHz and is further amplified using two room-temperature 30-dB amplifiers. A 3-dB attenuator is inserted between the amplifiers to avoid standing-waves and reflections. A DC voltage proportional to the signal intensity is obtained using a fast rectifier diode after the amplifier chain. The Y-factor is derived from measuring the AC and DC component from the voltage of the diode as a chopper periodically switches between the hot and cold load. The AC voltage component is measured using a lock-in which measures the rms value of the waveform. Since the waveform created by the chopper is approximately sinusoidal, the Y-factor is calculated

Fig. 3 of  $<0.1$  degrees translates to less than  $5 \mu\text{m}$  in the E-plane. The resulting displacement of the beam away from the central axis in the E-plane is, in this case, only a very small fraction of a degree. A displacement might also exist in the orthogonal direction, the H-plane, but currently we have no method of adjusting the dewar pitch angle in a controlled manner.

### C. RF Spectral Response

Prior to characterizing HEB mixer performance the RF spectral response has been checked using a Bruker IFS120HR Fourier-transform spectrometer. The center frequencies and bandwidths ( $\approx 50\%$ ) in general agreed with that expected for twin-slot antennas, indicating that the mixer RF spectral response is dominated by the planar antenna. The center frequency found experimentally for a twin-slot design at 600 GHz matches well with theory, however, a shift to lower frequencies of 20% is observed for designs at 2.5 THz<sup>[2]</sup>. A new twin-slot design, with a 10% reduction in the slot length was therefore fabricated to obtain a more desirable center frequency for the 2.5 THz measurements. The HEB was used as a direct detector for the spectral response measurements. In order to increase the HEB voltage responsivity, the device was operated at 6.9 K. Since, based on the design, the peak response was expected to occur around 2.5 THz, the spectra were measured using a  $23 \mu\text{m}$  Mylar beamsplitter which was judged to be ideal for the required frequency band: 1,200 GHz to 3,450 GHz (the Fabry-Perot resonances of the beamsplitter were outside of this band). The spectral response for antenna/RF-filter Type I (our first design), shown in Fig. 4, peaked at 2.0 THz having a somewhat asymmetric shape. The 10% shorter version, Type II (new design), not only displays the desired shift upwards in frequency, centered on 2.2 THz, but its shape is also more symmetric. At an LO frequency of 2.5 THz, Type II offers an increase of 1 dB in responsivity relative to Type I. Hence, the device geometry we have investigated has an slot length of  $0.28\lambda_0$  ( $\lambda_0$  is the free-space wavelength) and a RF-filter Type II. The large ringing present in the spectra, especially pronounced for the shorter slot antenna device, is due to standing waves in the device substrate. From the 164 GHz period of the undulations, the predicted substrate thickness is  $267 \mu\text{m}$  which is close to the nominal  $254 \mu\text{m}$  thickness specified by the wafer supplier. The 5 to 10% amplitude variations are due to the finite thickness of the cyanoacrylate adhesive that is used to glue the devices to the Si-lens. This adhesive is currently used since it readily dissolves in Acetone. If a less viscous adhesive, such as UV-curable optical glues, is substituted, this thickness would decrease and the standing wave pattern would be negligible.

### D. Intermediate Frequency Bandwidth Measurements at 630 GHz

A systematic study of the mixer 3-dB IF bandwidth on the HEB device length has been performed. The objective is to confirm that the  $1/L^2$  dependence, measured at low microwave frequencies<sup>[3]</sup>, holds as expected at submillimeter wave frequencies (where

these mixers will find practical applications). The IF bandwidths of HEB devices with lengths of 0.3, 0.2, and 0.1  $\mu\text{m}$  were measured. Figure 5 shows the results of two devices with dimensions  $L \times W = 0.1 \times 0.1 \mu\text{m}^2$ , which had a normal state resistance of 17  $\Omega$  and critical currents of 160 and 130  $\mu\text{A}$ . The data exhibits some scatter and periodic dips which we attribute to the interplay between the frequency sources, and also to reflections in the microstrip section. Since the two sources are not frequency locked together, the BWO displays a frequency drift on the order of 10 to 15 MHz. Although the IF spectrum is averaged during the measurement, the IF-power can vary by as much as  $\pm 1$  dBm over the 15 MHz span. The data points in the graph represent the average power throughout this band. Reflections are caused by impedance mismatch at the bonding wire transition from the device chip to the microstrip line and the solder joint between the microstrip line and the K-connector. From a 1-pole fit to the data, the 3-dB points are found to be 8.1 GHz and 9.2 GHz. The difference in the IF bandwidth could be caused by the choice of the bias point and physically different bridge lengths. The IF bandwidth of a  $0.08 \times 0.08 \mu\text{m}^2$  device has also been measured. The results showed no clear roll-off for frequencies up to 15 GHz. Due to the large scatter in the data, about 4 dB, this measurement result has not been included in the analysis of the length dependence.

In order to compare the experimental findings to theoretical predictions, the length and width of selected devices have been inspected using an SEM. The measured and "designed" sizes<sup>[10]</sup> are plotted together in Fig. 6. A trend is apparent that the length is about 20% longer and the width is about 20% narrower for the very smallest devices. Taking account of this correction the IF bandwidth has been plotted versus the actual bridge length in Fig. 7. The plot also includes our previous microwave results<sup>[3]</sup> for comparison. Using a electron diffusion-cooling limited model, the frequency roll-off is predicted to depend on the bridge length as:  $f_{3\text{dB}} = \pi D / 2L^2$ , where  $D$  is the diffusion coefficient and  $L$  is the device length. As seen in Fig. 7, the 630 GHz results fit the expected length dependence well. From the fit we find the diffusion coefficient to be 0.95  $\text{cm}^2/\text{s}$ , which is a reasonable result for a 120  $\text{\AA}$  thick Nb film<sup>[11]</sup>.

### E. Receiver Noise Temperature Measurements at 2.5 THz

In Fig. 8(a), a series of pumped I-V curves are shown when systematically varying the LO power of the 2.5 THz FIR-laser. For each of the curves, the optimal bias point resulting in the lowest receiver noise temperature, is indicated with a square marker. The position of the marker is consistently coincident with the knee in the I-V curve separating the normal state domain from the large differential resistance domain. The corresponding receiver noise temperature as function of the bias voltage is also shown - a characteristic parabolic shape is apparent.

Figure 8(b) shows the receiver noise as a function of LO power at 2.5 THz. The absorbed LO power is estimated using the "iso-thermal" method<sup>[12]</sup>. This method

assumes the HEB mixer element can be treated as a lumped element with a single electron temperature. The best result of  $1,800 \pm 100$  K was obtained for an absorbed LO power of 22 nW, at a bath temperature of 4.2 K. The large error bar for the noise temperature is due to laser power fluctuation during the measurement. These power fluctuations are due to oscillations between several transverse modes in the FIR laser, only one of which couples to the HEB mixer<sup>[13,14]</sup>. Efforts are underway to improve the stability of the FIR laser. This result is an improvement over our previous results<sup>[15]</sup> and is attributed primarily to the improved antenna design.

#### **F. Receiver Noise Temperature Measurements at 630 GHz**

The lowest stable receiver noise temperature achieved at 630 GHz was 470 K, as shown in Fig. 8(b), with an estimated absorbed LO power of 35 nW. Because of the stability of the local oscillator source (a BWO was used to pump the HEB mixer) chopping techniques were not needed during the measurement. For some LO power levels a lower receiver noise temperature (minimum was 320 K) was observed when biasing the device at a point of large or slightly negative differential resistance. However, biasing at a point of negative differential resistance should not be considered a viable operating point because of stability problems and fluctuations.

Figure 9 summarizes the DSB receiver noise temperatures available in the published literature to date. In this work we have been able to achieve the lowest receiver noise temperature for diffusion-cooled Nb HEB mixers at two frequencies: 630 GHz and 2.5 THz.

### **IV. SUMMARY**

This paper presents recent experimental results obtained with Nb HEB mixers having geometrical dimensions which makes diffusion the dominant cooling mechanism. A systematic study of the 3-dB IF bandwidth with length has shown the expected  $1/L^2$  dependence for the first time at submillimeter wave frequencies. In fact, a  $0.1 \mu\text{m}$  long device has given an IF bandwidth of 9 GHz, a receiver noise temperature of about 470 K, and an absorbed LO power of only 35 nW at 630 GHz. This is the largest IF bandwidth reported to date with extremely low receiver noise. In addition, by improving the mixer antenna and RF filter circuit, a receiver noise temperature of  $1800 \pm 100$  K has been achieved at 2.5 THz. This is the lowest noise to date obtained at this high frequency, and represents a significant improvement in the state-of-the-art for THz heterodyne mixers.

### **ACKNOWLEDGEMENT**

The authors are thankful to M.C. Gaidis for valuable contributions to the device design and acknowledge T. Crawford for the assistance with the use of the FTS for the antenna spectral response measurement. The research described in this paper was performed by the Center for Space Microelectronics Technology, Jet Propulsion Laboratory, California Institute of Technology, and was sponsored by the National Aeronautics and Space Administration, Office of Space Science.

## REFERENCES

- [1] A. Skalare, W.R. McGrath, B. Bumble, and H.G. LeDuc, "Measurements with a diffusion-cooled Nb hot-electron bolometer mixer at 1100 GHz," *Proc. of the 9th Int. Symp. on Space THz Tech.*, pp. 115-120, Jet Propulsion Laboratory, Pasadena, CA (1998).
- [2] B.S. Karasik, M.C. Gaidis, W.R. McGrath, B. Bumble, and H.G. LeDuc, "A low-noise 2.5 THz superconductive Nb hot-electron mixer," *IEEE Trans. Appl. Supercond.* **7** (2), 3580 (1997).
- [3] P.J. Burke, R.J. Schoelkopf, D.E. Prober, A. Skalare, W.R. McGrath, B. Bumble, and H.G. LeDuc, "Length scaling of bandwidth and noise in hot-electron superconducting mixers," *Appl. Phys. Lett.* **68** (23), 3344 (1996).
- [4] J. Schubert, A. Semenov, G.N. Gol'tsman, H.-W. Hübers, G. Schwaab, B. Voronov, and E. Gershenzon, "Noise temperature and sensitivity of a NbN hot-electron mixer at 2.5 THz," *Proc. of the 10th Int. Symp. on Space THz Tech.*, University of Virginia, Charlottesville, VA (1999).
- [5] E. Gerecht, C.F. Musante, H. Jian, Y. Zhuang, K.S. Yngvesson, J. Dickinson, T. Goyette, J. Waldman, P. Yagoubov, G.N. Gol'tsman, B.M. Voronov, and E.M. Gershenzon, "Improved characteristics of NbN HEB mixers integrated with log-periodic antennas," *Proc. of the 10th Int. Symp. on Space THz Tech.*, University of Virginia, Charlottesville, VA (1999).
- [6] P. Yagoubov, M. Kroug, H. Merkel, E. Kollberg, J. Schubert, H.-W. Hübers, G. Schwaab, G.N. Gol'tsman, and E.M. Gershenzon, "NbN hot electron bolometric mixers at frequencies between 0.7 and 3.1 THz," *Proc. of the 10th Int. Symp. on Space THz Tech.*, University of Virginia, Charlottesville, VA (1999).
- [7] B. Bumble and H.G. LeDuc, "Fabrication of a diffusion cooled superconducting hot electron bolometer for THz mixing applications," *IEEE Trans. Appl. Supercond.* **7** (2), 3560 (1997).

- [8] Zitex A-135, Norton Performance Plastics Corp., Wayne, NJ.
- [9] D.F. Filipovic, S.S. Gearhart, and G.M. Rebeiz, "Double-slot antennas on extended hemispherical and elliptical silicon dielectric lenses," *IEEE Trans. on Microwave Theory Tech.* **41** (10), 1738 (1993).
- [10] P.M. Echternach, H.G. LeDuc, A. Skalare, and W.R. McGrath, "Fabrication of an Aluminum based hot electron mixer for terahertz applications," *Proc. of the 10th Int. Symp. on Space THz Tech.*, University of Virginia, Charlottesville, VA (1999).
- [11] B.S. Karasik, K.S. Il'in, E.V. Pechen, and S.I. Krasnosvobodtsev, "Diffusion cooling mechanism in a hot-electron NbN microbolometer," *Appl. Phys. Lett.* **68** (16), 2285 (1996); and references therein.
- [12] H. Ekström, B.S. Karasik, and E. Kollberg, "Conversion gain and noise of Niobium superconducting hot electron mixers," *IEEE Trans. Microwave Tech.* **45** (4), 938 (1995); for a more precise method see H. Merkel, P. Yagoubov, P. Khosropanah, and E. Kollberg, "An accurate calculation method of the absorbed LO power in hot electron bolometric mixers," *IEEE 6th Int. Conf. On THz Elec. Proc.*, Leeds, UK, September 1998, pp. 145-148.
- [13] H.P. Röser, M. Yamanaka, R. Wattenbach, and G.V. Schultz, "Investigation of optically pumped submillimeter wave laser modes," *Int. J. Infrared and Millimeter Waves* **3** (6), 839 (1982).
- [14] R. Wattenbach, H.P. Röser, and G.V. Schultz, "A microprocessor stabilized submillimeter laser system," *Int. J. Infrared and Millimeter Waves* **3** (5), 753 (1982).
- [15] B.S. Karasik, M.C. Gaidis, W.R. McGrath, B. Bumble, and H.G. LeDuc, "Low noise in a diffusion-cooled hot-electron mixer at 2.5 THz," *Appl. Phys. Lett.* **71** (11), 1567 (1997).
- [16] A. Skalare, W. R. McGrath, B. Bumble, H. G. LeDuc, P. J. Burke, A. A. Verheijen, R. J. Schoelkopf, D. E. Prober, "Large bandwidth and low noise in a diffusion-cooled hot electron bolometer mixer," *Appl. Phys. Lett.* **68**, 1558 (1996).

## FIGURES

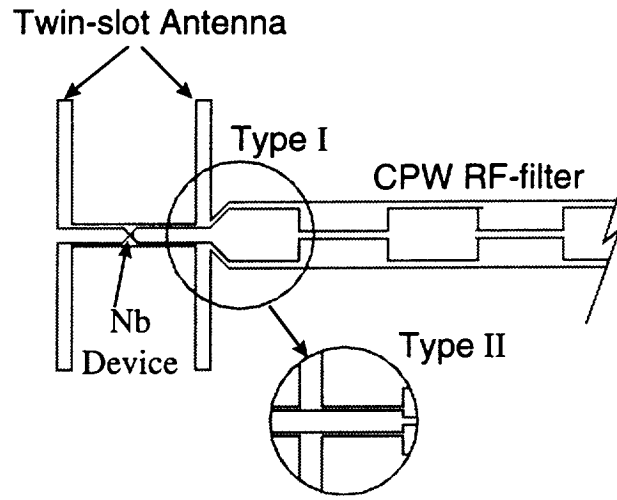


FIG. 1. Layout of HEB mixer circuit. Two slot lengths,  $0.31\lambda_0$  and a 10% reduced version measuring  $0.28\lambda_0$  (where  $\lambda_0$  is the free space wavelength), together with two variations of the first section of the rf bandstop filter, Type I and Type II, have been implemented.

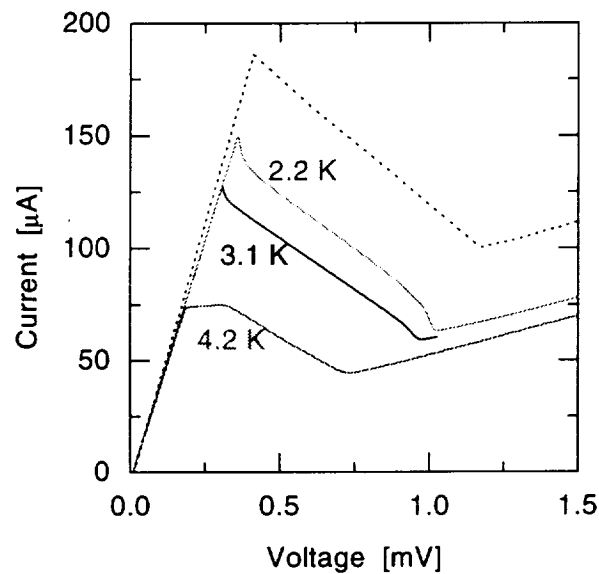


FIG. 2. DC I-V characteristics of a Nb HEB device measured during the initial dipstick test into LHe (dashed line) and three months later after multiple mountings in the mixer block (solid line). Note the decrease of the critical current from 186  $\mu\text{A}$  to 74  $\mu\text{A}$  at 4.2 K, which is partially recovered when lowering the bath temperature to 2.2 K (150  $\mu\text{A}$ ).



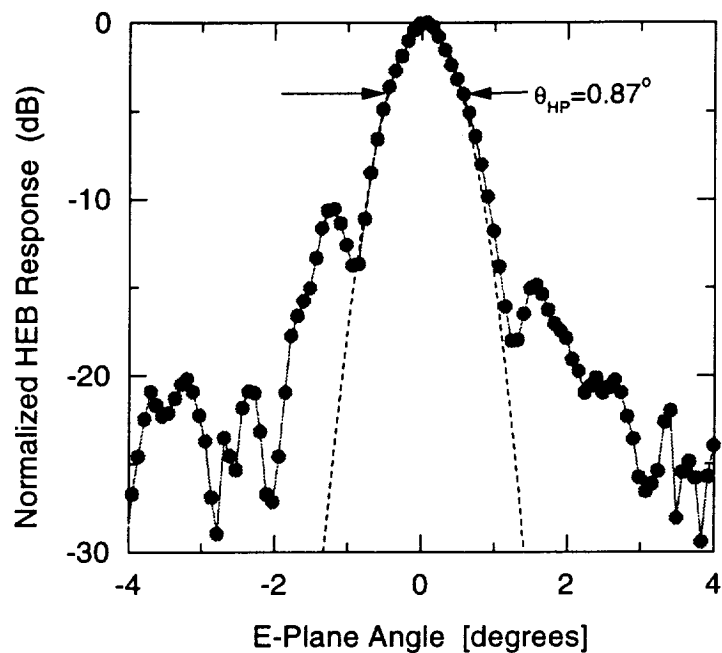


FIG. 3. Measured E-plane beam pattern at 2.5 THz receiver with HEB operated as a direct detector.

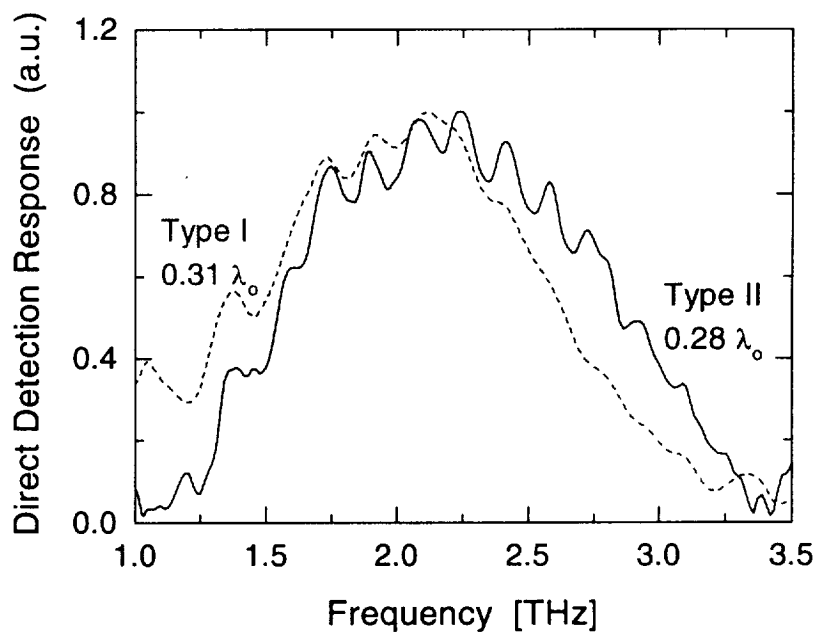


FIG. 4. RF-response of HEB mixer. A spectral resolution of  $1 \text{ cm}^{-1}$  was used during the measurement with the Fourier-transform spectrometer.

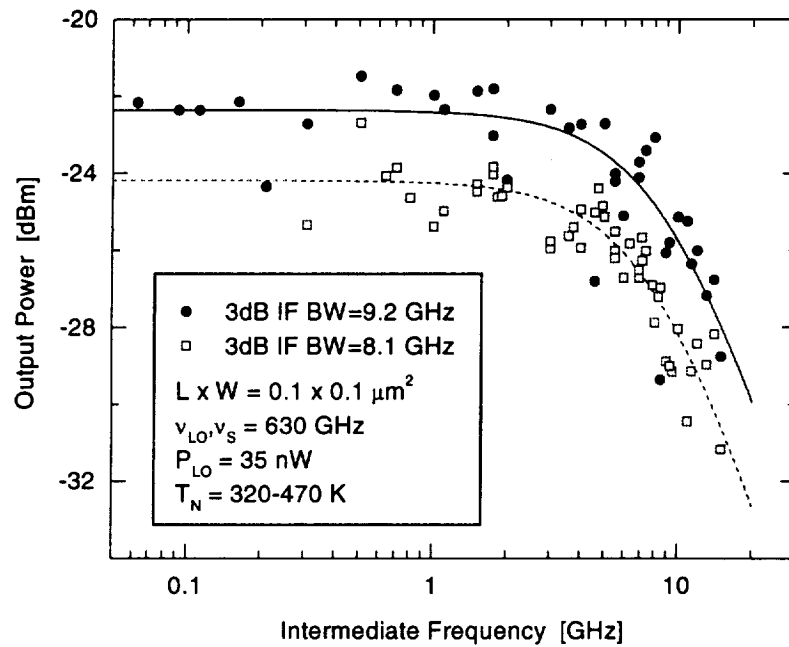


FIG. 5. Relative SSB conversion efficiency vs. intermediate frequency for two different HEB devices with 600 GHz twin-slot antennas.

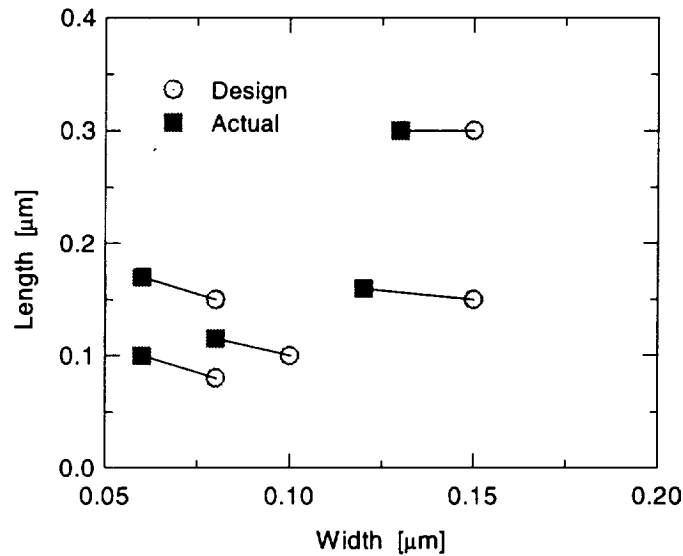


FIG. 6. Design and actual dimensions of Nb microbridge. The actual dimensions are found by visual inspection of SEM photographs.

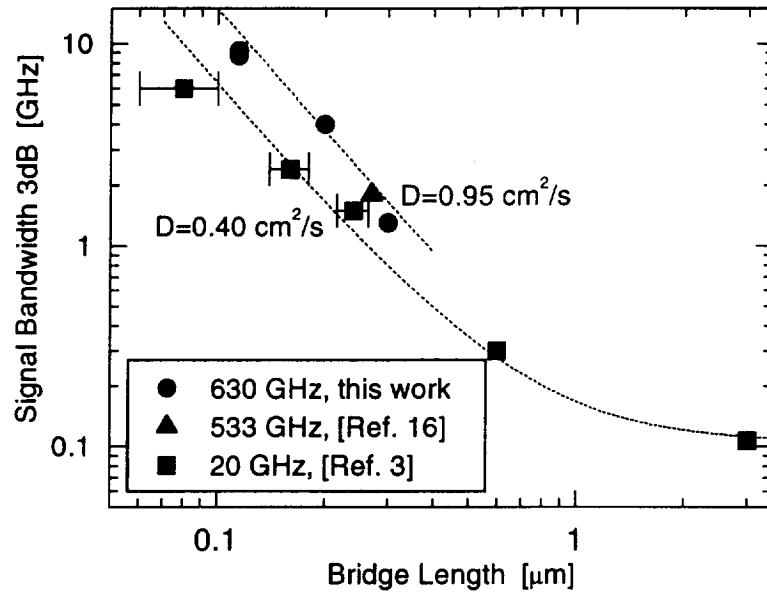


FIG. 7. Scaling of signal bandwidth with device length.

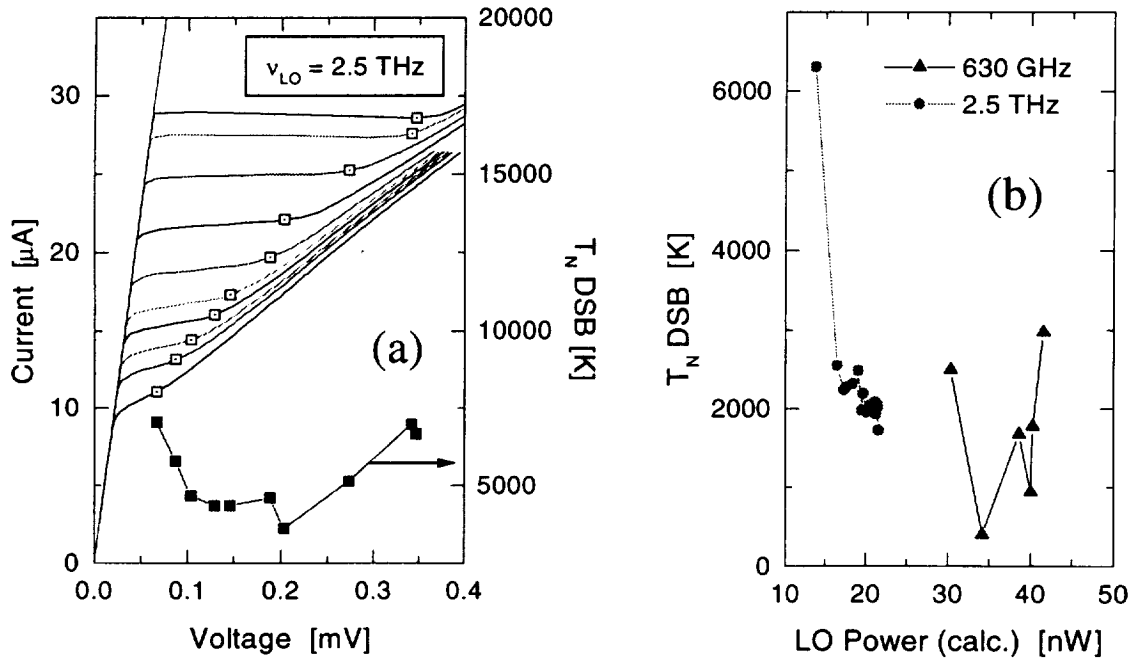


FIG. 8. (a) Pumped DC I-V of HEB mixer for increasing LO power levels at 2.5 THz. The square symbol indicates the optimal bias point to achieve the lowest DSB noise temperature. (b) DSB noise temperature of HEB mixer vs. the estimated absorbed LO power.

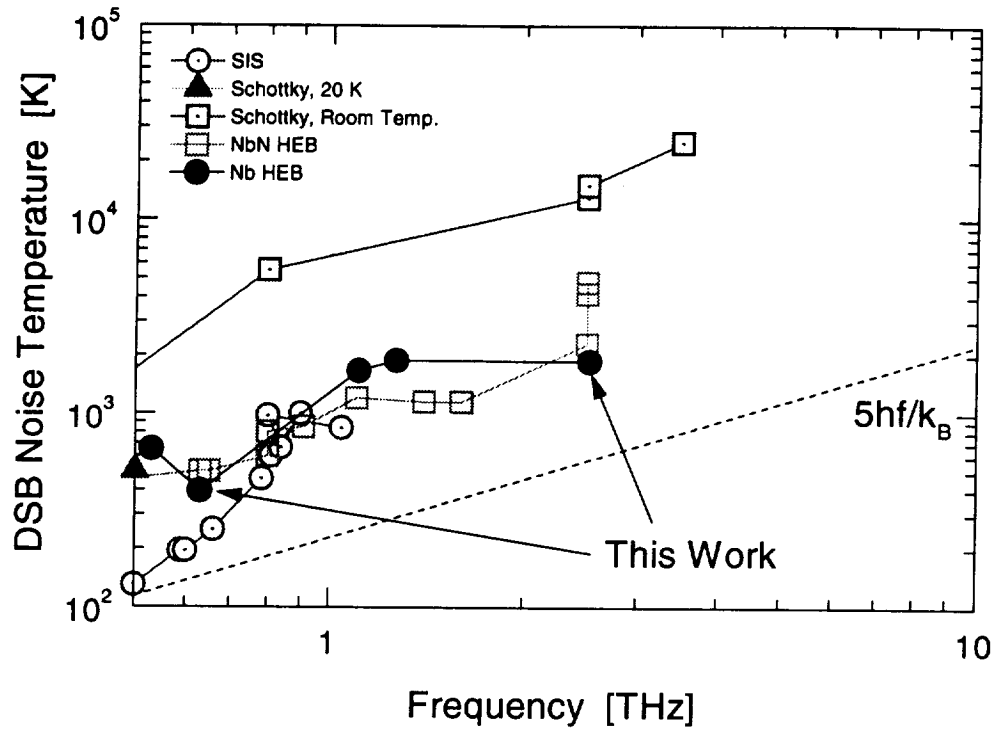


FIG. 9. The graph gives a summary of the currently reported DSB noise temperatures of competing heterodyne receiver technologies. In the graph, the most recent results, 320-470 K at 630 GHz and 1800±100 K have been included.